HIGHLY EFFICIENT HYDROGEN EVOLUTION BY USING $Zn_{1-X}Cd_XS$ COMPOSITES DERIVED METAL ORGANIC FRAMEWORK UNDER VISIBLE LIGHT ILLUMINATION

Pyai Pyai Phyo[1], Tian Liang[2]

Abstract

Hydrogen production from water splitting under visible-light irradiation is considered as an ideal process to convert solar energy into renewable hydrogen energy and a promising technology to reduce fossil fuel consumption. In this research, $Zn_{1-X}Cd_XS$ derived metal organic framework was developed via an elementary hydrothermal method that was integrated with the calcination means. The different experimental parameters were employed to investigate the transformation of phase and morphology. The $Zn_{0.7}Cd_{0.3}S$ nano material exhibited the higher hydrogen production rate of 14.1 mmol $h^{-1}g^{-1}$ under cocatalyst-free and visible-light irradiation conditions. Furthermore, these ZnCdS nano materials showed excellent long-term stability, maintaining high photocatalytic activity for hydrogen evolution over a number of cycles. This research work represents a simple strategy to fabricate visible-light responded ZnCdS derived from zeolitic-imidazolate-framework-8 (ZIF-8) and highlights the critical role for developing Z-scheme photocatalyst in solar energy conversion.

Keyword: hydrothermal method, metal organic framework, hydrogen evolution, photocatalyst

Introduction

The problems of the global energy crisis and environmental pollution insist on clean and renewable energy alternatives. Photo-catalytic hydrogen evolution from water splitting by using sun light and a photocatalyst has been considered as an ideal process to convert solar energy into chemical energy and as a promising technology to reduce fossil fuel consumption. Photocatalytic water splitting is a process that requires only light energy, water and a catalyst for dissociation of water into hydrogen and oxygen. In particular, hydrogen production using solar energy has attracted significant attention as a key issue in the utilization of the sun as the most abundant renewable energy source. Hydrogen is a clean energy carrier when used in fuel cells because only water is emitted as an oxidation product.

Nowadays, numerous semiconductor-type photocatalysts (e.g., oxides, sulfides, and oxynitride semiconductors) are being explored as one class of the most promising low-cost catalysts for producing hydrogen energy under visible light irradiation ($\lambda > 420$ nm) (Y. J. Yuanet.al, 2016). The photocatalytic splitting of water into hydrogen and oxygen by using a powdered photocatalyst has become the subject of research, mainly focusing on the visible light sensitization of photocatalysts because visible light accounts for about 45 % of sunlight. In this research work, a ZnCdS rhombic dodecahedral structure by employing zeolitic-imidazolate-framework-8 (ZIF-8), a metal-organic frameworks (MOFs), which are constructed through coordination bonds between metal ions/clusters and organic ligands, an attractive nanoporous crystalline material for a variety of potential applications due to its unique structural and physicochemical properties. The as-prepared hollow ZnCdS cages showed significantly enhanced activity and durability in photocatalytic water splitting without any co-catalyst and photosensitizer under visible-light illumination. By adjusting the Cadmium (Cd) content of the

[1] Department of Industrial Chemistry, East Yangon University, Yangon.
[2] Department of Environmental Science and Chemical Engineering, Shanghai University, China.

$Zn_{1-X}Cd_XS$, the chemical composition of the $Zn_{1-X}Cd_XS$ catalysts can be fine-tuned to optimize the light absorption capacity, charge carrier separation efficiency and photocatalytic activity by controlling the conduction band edge of the catalyst (X. Zhao, 2018).

Materials and Methods

Chemicals

Zinc nitrate hexahydrate Zn $(NO_3)_2$. $6H_2O$, 2-methylimidazole ($C_4H_6N_2$), thioacetamide (TAA) and methanol were purchased from Sinopharm Group Chemical Reagent Co., Ltd, China. Cadmium acetate dihydrate Cd $(CH_3COO)_2.2H_2O$, ethanol and ethylene glycol from Adamas Reagent Co., Ltd, China.

Synthesis of ZIF-8 Nanoparticle

ZIF-8 nanoparticle was synthesized according to the method previously reported in literatures. Specific method is as follows: 1.8 g of zinc nitrate hexahydrate (Zn $(NO_3)_2.6H_2O$ containing Zinc (Zn, 6.05 mmol) and 3.96 g of 2-methylimidazole ($C_4H_6N_2$, 48.23 mmol) were separately dissolved in 67.8 g of methanol. The two solutions were rapidly mixed into a glass beaker (300 mL); then a white powdery solid was obtained after stirring for one hour at room temperature. The solid product was centrifuged (4000 rpm, 10 min) and washed with methanol for purification. This procedure was repeated twice. Finally, the resultant ZIF-8 powder was dried in a vacuum drying oven overnight at 80 ℃, then stored in a desiccator before using.

Preparation of the $Zn_{1-X}Cd_XS$ Nanomaterials

The hollow ZnCdS materials were obtained by using ZIF-8 as the precursor. Firstly, hollow ZnS was prepared by the sulfurization of ZIF-8. Briefly, thioacetamide (TAA) (500 mg) was dissolved in 10 mL ethanol. ZIF-8 was mixed with the above solution and treated at 40 ℃ for 24 h under stirring. Then, the obtained hollow ZnS and a certain amount of cadmium acetate dihydrate Cd $(CH_3COO)_2.2H_2O$ were added to 20 mL of ethylene glycol under continuous stirring. After 30 min of continuous stirring, the aqueous solution was transferred to a 100 mL Teflon-lined stainless-steel autoclave as shown in Figure (1) and heated at 160℃ for 4 h in the oven. The resulting hollow ZnCdS was collected via centrifugation, washed thoroughly with ethanol, and dried under vacuum at 40 ℃ for 12 h. By adjusting the amount of Cd $(CH_3COO)_2.2H_2O$, $Zn_{1-x}Cd_xS$ (x= 0, 0.1, 0.3, 0.5, 0.7, 0.9) nanomaterials can be obtained.

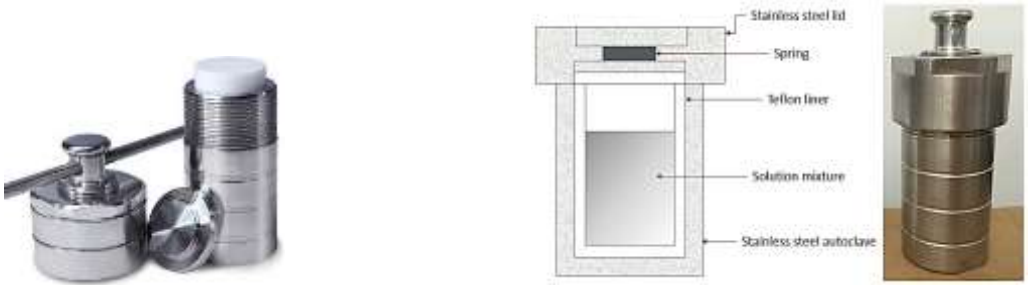

Figure 1: Teflon-lined Stainless-Steel Autoclave

Results and Discussion

Powder X-ray diffraction (XRD) patterns were collected by using by a Bruker D 8 advance X-ray diffractometer that used Cu K α radiation and the diffraction patterns were recorded over the 2θ range of 5-80° with scan rate of 5 min^{-1}. According to Figure 2 (a), the characteristic peak ZIF-8 almost corresponds with the stimulated data from the standard card JCPDS(No.864310).

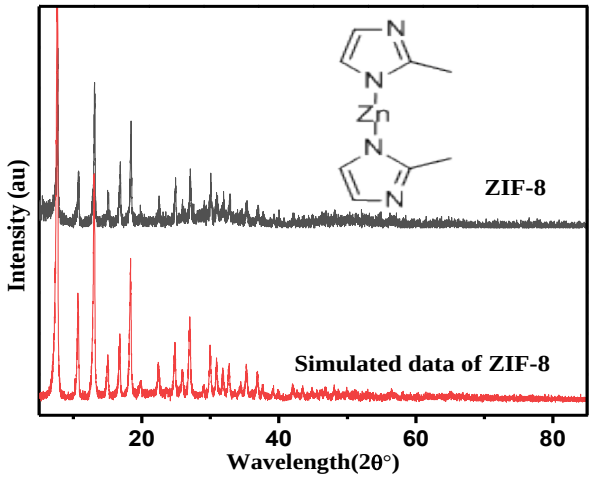

Figure 2: (a) XRD Patterns of ZIF-8

Furthermore, XRD patterns of the hollow $Zn_{1-x}Cd_xS$ with different metal ratios are shown in Figure 2 (b). The XRD pattern of Zn $_{1-x}Cd_xS$ in Figure 2 (b) is consistent with the standard card JCPDS NO.40-0985, indicating that the synthesized $Zn_{1-x}Cd_xS$ crystallinity is relatively high. As compared to the hollow ZnS, the XRD peak positions for $Zn_{1-x}Cd_xS$ were slightly shifted to lower degrees, i.e., from 39.5 to 35.2, 34.9, 33.9 and 33.6, respectively, as the content of Cd increased (x = 0.1, 0.3, 0.5, 0.7 and 0.9) and indicated that an expansion to a higher lattice parameter. This observation suggests the formation of solid solutions rather than simple physical mixtures of ZnS and CdS.

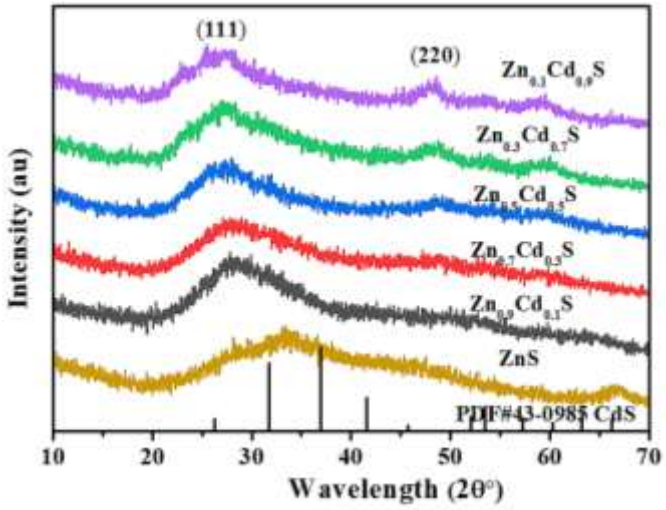

Figure 2: (b) XRD Patterns of the As-synthesized $Zn_{1-x}Cd_xS$ with Different Metal Ratios

The morphologies of the as-prepared ZIF-8 and hollow $Zn_{1-x}Cd_xS$ with different metal compositions were characterized by the SEM images which were performed on Hitachi FESEM-4800. Figures 4 (a) and (b) show the SEM images of ZIF-8 and Figures 4 (c) and 4 (d) are the composite of $Zn_{0.7}Cd_{0.3}S$. The SEM images of ZIF-8 showed highly uniform and well-dispersed rhombic dodecahedral particles. In Figures 4(c) and 4(d), the appearance of composite $Zn_{0.7}Cd_{0.3}S$ has a rhombic shape and the surface is rough and uneven.

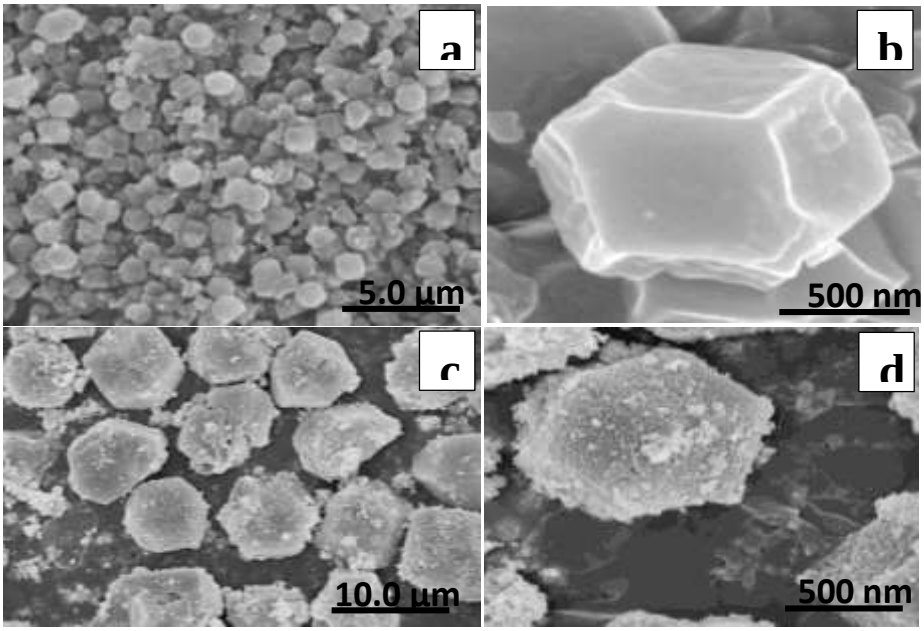

Figure 3: (a) and (b) SEM Images of ZIF-8
(c) and (d) SEM Images of $Zn_{0.7}Cd_{0.3}S$ Composites

Photocatalytic Tests

The photocatalytic hydrogen experiments were conducted in a gas-closed circulation system (CEL-SPH2N) and connected to an on-line gas chromatograph (GC-8A, CEALJ LIGHT) with a thermal conductivity detector (TCD) for fully automated hydrogen detection. The gas in the gas-closed circulation system is automatically extracted into the gas chromatograph system at a set interval, and the specific volume of the produced hydrogen gas can be determined by the peak area through the standard curves. According to a conventional method, 50 mg of the catalyst was weighed and added into a reactor containing 50 mL of deionized water containing 20 % CH_3OH that acts as a sacrificial agent, and continuously stirred by a magnetic stirrer. The low temperature condition of 20 ℃ is controlled by the cooling circulating water system. The light source system is a 300 W Xe lamp (CEL-HXF 300). The hydrogen production by photocatalysis in the laboratory is presented in Schematic Diagram of Figure (4).

Photocatalytic Performance

The photocatalytic hydrogen production experiment was carried out under a visible light irradiation ($\lambda > 400$ nm) with methanol as a sacrificial agent. As shown in Figure 5 (a), the hydrogen yield was negligible when pure ZnS was used as a photocatalyst, owing to its poor visible light absorption. After the introduction of Cd atoms, the activity of $Zn_{1-x}Cd_xS$ was dramatically enhanced. Moreover, the efficient hydrogen production ability of ZnCdS nanocomposites could be well controlled by changing the contents of Cd. The average hydrogen

evolution rate on 3 h for each composite as shown in figures 5 (a) and 5 (b). According to these results, $Zn_{0.7}Cd_{0.3}S$ represented the highest catalytic activity with an average H_2 production rate of 14.1 mmol h^{-1} g^{-1}, ranking among the reported ZnCdS photocatalysts under cocatalyst-free and visible light irradiation ($\lambda > 420$ nm) conditions. This superior photo-catalytic water splitting performance was even beyond that of some sulphide-based catalysts loaded with noble metals as co-catalysts.

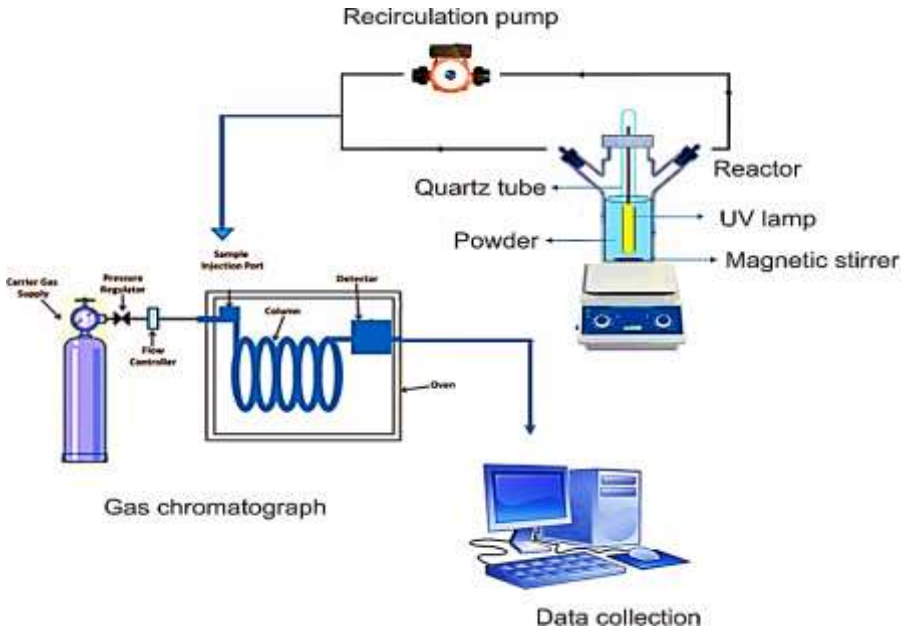

Figure 4: Schematic Diagram of the Reaction System for Hydrogen Production by Photocatalysis

The optical absorption capability of a photocatalyst may have essential impacts on its photocatalytic activity. In this regard, the optical properties of $Zn_{1-x}Cd_xS$ composites were investigated by solid UV-visible diffuse reflectance spectroscopy (UV-Vis DRS). As shown in Figure 6 (a), the as-prepared hollow ZnS cages represented a broad absorption band that extended from the ultraviolet to the near-ultraviolet range and a steep absorption edge. This result was indicative of high phase purity and crystallinity of the hollow material with a uniform structural morphology. The obvious shift of the absorption edges and a significant increase of the absorption intensity in the wavelength region shorter than 520 nm, could be detected with increasing Cd content in the $Zn_{1-x}Cd_xS$ composites.

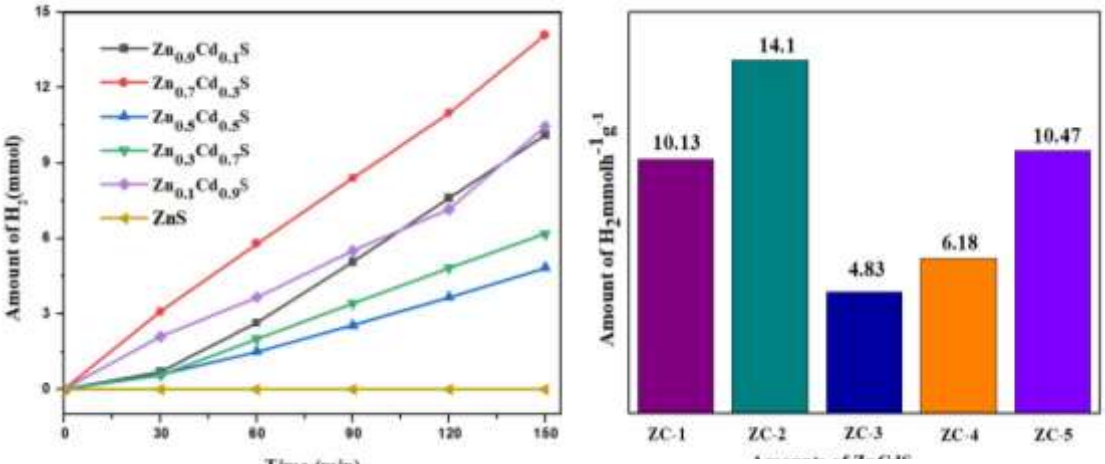

Figure 5: (a) Photocatalytic Hydrogen Generation of $Zn_{1-x}Cd_xS$ Composites (b) Average Hydrogen Evolution Rate of $Zn_{1-x}Cd_xS$ Composites for 3 h

The bandgap energy (Eg) of the as-synthesized ZnS and $Zn_{1-x}Cd_xS$ samples could be estimated from these spectra according to the Kubelka–Munk method using the following equation:

$$\alpha h\nu = A(h\nu - E_g)^{1/2}$$

where α is the absorption coefficient, A is a constant, *hν* is the photon energy and h is Planck's constant. (K. Zhang.et al., 2016). The results are shown in Table (1). The UV-Vis Absorption Spectrum of ZnS and E_g value (3.15eV) of ZnS is shown in Figure 6 (a) and (b). Furthermore, the E_g value of Zn $_{1-x}Cd_xS$ composites varied from 2.34 eV to 2.14 eV, representing mostly a decreasing trend by varying Cd content as shown in Figures 7 (a) and 7 (b). These results indicated that the introduction of Cd atoms into the ZnS structure could significantly lower the E_g values. The data represented that it is more effective harvest of visible light, consequently, implying that these MOF-derivatives might have good visible-light photocatalytic activities. The photocatalytic hydrogen production activity of the as-prepared $Zn_{1-x}Cd_xS$ and its related samples for control experiments were investigated under visible light irradiation (λ > 420 nm) for 3 h in the absence of any cocatalyst.

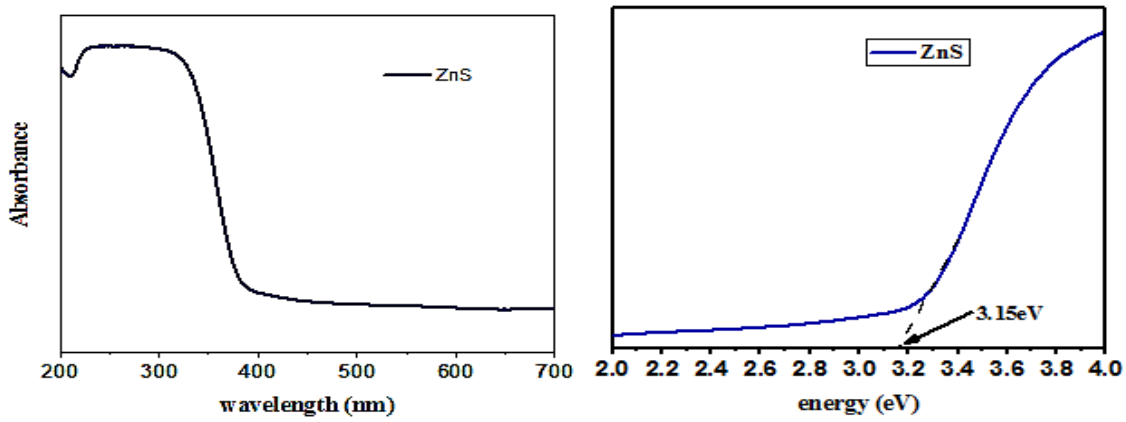

(a) (b)

Figure 6: (a) UV-Vis Absorption Spectrum of ZnS derived from ZIF-ʊ
(b) Curve of Kubelka-Munk Function Plotted Against the Photon Energy

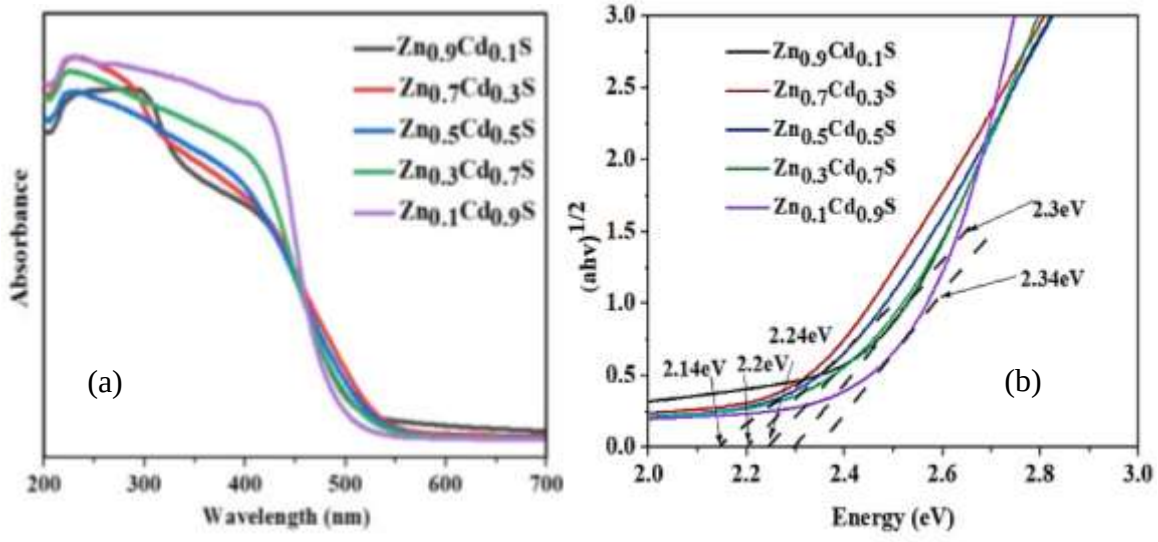

Figure 7: (a) UV-Vis Absorption Spectra of $Zn_{1-x}Cd_xS$ Nanocomposites
(b) Curve of Kubelka-Munk Function Plotted Against the Photon energy

Table 1. Properties of $Zn_{1-x}Cd_xS$ Composites

Sr.No	Catalysts	E_g(eV)	HER (mmol $g^{-1}h^{-1}$)
1.	ZnS	3.15	-
2.	$Zn_{0.9}Cd_{0.1}S$	2.3	10.13
3.	$Zn_{0.7}Cd_{0.3}S$*	2.34	14.1
4.	$Zn_{0.5}Cd_{0.5}S$	2.14	4.83
5.	$Zn_{0.3}Cd_{0.7}S$	2.24	6.18
6.	$Zn_{0.1}Cd_{0.9}S$	2.2	10.47

Conclusion

In conclusion, a metal–organic framework (MOF) template strategy with hydrothermal sulfidation and thermal annealing was successfully developed to fabricate $Znx_{-1}Cd_xS$ for photocatalytic H_2 evolution under visible light irradiation. Turnability of the $Zn_{x-1}Cd_xS$ energy band was realized via changing Cadmium (Cd) concentrations and the optimal photocatalytic activity is primarily influenced by structural and morphological superiorities. ZnCdS catalysts also showed excellent chemical and thermal stability and catalytic durability, suggesting that their great potential in practical applications. In addition, the construction of hollow ZnCdS cages by using MOFs as precursors might bring new opportunities in developing highly effective and durable photocatalysts for a wide range of photochemical applications.

Acknowledgements

I would like to express my profound gratitude to the Myanmar Academy of Arts and Science for permitting to publish this paper. I would first like to express my sincere gratitude to Dr. Nay Win Oo, Rector of East Yangon University, Dr. Aye Aye Ko, Dr. War War Lwin, Dr. Thida Aung, Pro-Rectors of East Yangon University and to professor Dr. Moe Theingi Hlaing, Head of Department of Industrial Chemistry, East Yangon University for their kind encouragement. I would like to express my deepest gratitude to Dr. Tian Liang, Professor, Department of Environmental Science and Chemical Engineering, Shanghai University, China for his suggestions and valuable advices as a supervisor.

References

C. Jianmin, Junying C. and Yingwei L. (2017) Hollow ZnCdS dodecahedral cages for highly efficient visible-light-driven hydrogen generation, Journal of Materials Chemistry A.

C. Xing, Zhang Y., Yan W. and Guo L., 2006, Band structure-controlled solid solution of $Cd_{1-x}Zn_xS$ photocatalyst for hydrogen production by water splitting, International Journal of Hydrogen Energy, Volume31.

E. Patterson, C. Shelden, B. Stockton, 2020, An Efficient and Stable $MoS_2/Zn_{0.5}Cd_{0.5}S$Nanocatalyst for Photocatalytic Hydrogen Evolution, Journal of chemistry in Europe, 26-53, 12206-12211.

K. Zhang, Wang L., and Park J. H., (2016) An order/disorder/water junction system for highly efficient co-catalyst-free photocatalytic hydrogen generation, Journal of Energy and Environmental Science, Issue 2.

K.S. Park, Ni Z., Côté A.P, Choi J.Y., R. Huang, O'Keeffe M.and Yaghi O.M., (2006), Exceptional chemical and thermal stability of zeolitic imidazolate frameworks, National Academic of Science U.S.A.

N. Serpone, D. Lawless, R. Khairutdinov, J.,1995, Size Effects on the Photophysical Properties of Colloidal Anatase TiO_2 Particles: Size Quantization Versus Direct Transitions in This Indirect Semiconductor, the Journal of Physical Chemistry,99,16646-16654.

X. Zhao, Jianrui F., Jing L., Wei S., Guangming Y., Gui-Chang W., and Peng C. (2018) An Efficient, Visible-Light-Driven, Hydrogen Evolution Catalyst $NiS/Zn_xCd_{1-x}S$ Nanocrystal Derived from a Metal–Organic Framework, Journal of German Chemical Society, Volume 57.

Yuan Y. J., Tu J. R., Ye Z. J., Huang Y. W., D. P. Cao, Z. T. Yu and Z. G. Zou, (2016), MoS_2-graphene/$ZnIn_2S_4$ hierarchical microarchitectures between light-harvesting semiconductor and cocatalyst for solar hydrogen generation Applied Catalysis B: Journal of Environmental Science. 188: pp. 13-22**.**